УДК 531.38

©2003. **N.V. Khlistunova**

SYMPLECTIC INTEGRATION FOR THE EULER CASE OF MOTION OF A NEARLY SYMMETRIC RIGID BODY

In this paper a new approach useful for numerical integration of the motion equations for a free rigid body with a fixed point is studied. The approach employs symplectic integration schemes of the second and third order. These schemes are presented as a sequence of rotations with two frequencies per each integration step. Both schemes are implemented and tested against Runge-Kutta-Fehlberg fifth order method, the represented computational results are satisfactory.

Introduction. In space applications such as attitude and orbital control of artificial satellites the practical implementation of control often cause a need in precise numerical integration of main variables characterizing the satellite motion. For small and cheap satellites the budget cost of payload is a reason to put some restrictions on the satellite design, for example, the bounds on the mass. Due to strong solar radiation on the orbit the mission safety also restricts the configuration of the main onboard computer to low frequency models like Intel 80386. Long computational time usual for that models gives rise to the question of choice of the fastest numerical method. Thus the integration method has to be as fast as accurate and give satisfactory results for long term predictions.

Modern theory of numerical methods for ordinary differential equations (ODEs) systems allows to satisfy all those requirements by choosing an algorithm with good efficiency, even comparable to a complicated approximate solution expressed in terms of special mathematical functions. Nowadays, for example, symplectic integration methods are successfully applied to various Hamiltonian systems [1-4]. To provide fast computation and good accuracy symplectic methods are constructed to use integrable parts of the force field and geometric behavior of Hamiltonian systems.

In celestial mechanics for the planetary n-body problem the symplectic integrator was presented by Wisdom and Holman [1] and then used by Wisdom and Sussman [2] to integrate the evolution of the whole solar system for long time period. The symplectic method for integration the motion equations of a free rigid body, which conserves the magnitude of angular momentum vector and is accurate to the first order of the time step, was introduced in [3]. Then gravitational interacting of the body with mass points was incorporated into dynamics to generate the symplectic scheme which conserves the total angular momentum of the system. It was confirmed that the presented integrators provide high precision and fast computation. The book [4] by Sanz-Serna and Calvo represents extensive numerical experiments with symplectic integration applied to different Hamiltonian systems like Henon-Heiles and Kepler problems. In the area of satellite orbit dynamics the paper [5] shows the practical effectivness of symplectic integration technique which has been incorporated into a batch filter to solve the orbit estimation problem.

This paper expands application of symplectic integrators of the second and third order in the problem of attitude dynamics of small satellite rotating about a fixed point on orbital trajectory. The most simple model to begin the study with, concerns the propagation of angular velocity of a free rigid body rotating about the mass center as the fixed point. Then

according to the well-known Euler integrability case the motion equations are integrated in quadratures and expressed in terms of elliptical Jacobi functions. However, the calculation of Jacobi function can be time consuming operation for the computer in hand. Fortunately, the symplectic approach is applicable for this problem because of the practical and theoretical features formulated next. Indeed, many of small satellites have nearly axisymmetric mass distribution and this fact eliminates the particular Euler case of regular precession about one of principal inertia axes among different rotational regimes. In such a case the hodograph of angular velocity is easily propagated in terms of trigonometric functions. Following [3], in this paper the corresponding exact solution is used to construct the symplectic schemes of the second and third order. The angular dynamics of the body can be further complicated by introduction of disturbances due to Earth gravity and magnetic fields, but these issues will be left to the future work.

1. Splitting methods for numerical integration of ODEs. It is often difficult to find analytically general exact solution for ODEs system, however numerical integration allows to compute particular solution for the initial value given. Splitting methods for numerical integration of ODEs system are especially effective when the force field can be divided into two or more integrable parts. This is also shared by symplectic methods. It is assumed that the autonomous system of ODEs is written in the form

$$\dot{\mathbf{X}} = \sum_{k=1}^{m} \mathbf{F}_k(\mathbf{X}), \tag{1}$$

where $\mathbf{X} \in \mathbf{R}^n$, the vector-functions, $\mathbf{F}_k = (\mathbf{F}_1^k, \ldots, \mathbf{F}_n^k)$ $(k = 1, \ldots, m)$, represent the parts of the acting force field. The initial conditions are

$$\mathbf{X}(t_0) = \mathbf{X}_0. \tag{2}$$

The advantageous feature of splitting methods permits to construct easily the approximate numerical solution for (1),(2), without application any of conventional ODEs integrators as, for example, Runge-Kutta methods. The assumption, that the vector-functions $\mathbf{F}_k$ are linear on $\mathbf{X}$, provides the existence and uniqueness of exact solutions for the initial value problems

$$\dot{\mathbf{X}} = \mathbf{F}_k\mathbf{X}, \qquad \mathbf{X}(t_0) = \mathbf{X}_0, \quad (k = 1, \ldots, m), \tag{3}$$

then the corresponding solutions are given explicitly

$$\mathbf{X}_k(t) = \mathbf{X}_0 \exp(\mathbf{F}_k t). \tag{4}$$

Next, all the solutions, $\mathbf{X}_k(t)$ $(k = 1, \ldots, m)$, are composed into the approximate solution for (1),(2). According to the Baker - Campbell - Hausdorff formula the general operator exponent is the composition

$$\exp(A + B) = \exp(C), \tag{5}$$

$$C = \sum C_i = A + B + \frac{1}{2}\{A, B\} + \frac{1}{12}\{A, A, B\} + \frac{1}{12}\{B, B, A\} + \frac{1}{24}\{A, B, B, A\} + \ldots, \tag{6}$$

here $\{A, B\} = AB - BA$ designate the commutator brackets of two linear noncommutative operators A and B. If the first order accuracy is satisfactory, then, based on (3)-(6), the approximate solution of (1),(2)is

$$\mathbf{X}(t) = \mathbf{X}_0 \left(\exp\Big(\sum_{k=1}^{m} \mathbf{F}_k t \Big) + O(t^2) \right). \tag{7}$$

Therefore, the composition of exact solutions (4) results in explicit procedure (7) of numerical integration of the ODE system called as the splitting method.

For Hamiltonian systems the exact solutions are symplectic maps (i.e. canonic). If it is assumed that two sets of the canonic variables $(\mathbf{q},\mathbf{p}) \in R^{2n}$ and $(\mathbf{q}^*,\mathbf{p}^*) \in R^{2n}$ are given for Hamiltonian system considered, then the definition of symplectic mapping [4] can be introduced as following.

Definition. The mapping $G : (\mathbf{q},\mathbf{p}) \to (\mathbf{q}^*,\mathbf{p}^*)$ is called symplectic, if its Jacobian matrix $(2n \times 2n)$ satisfies to the relation

$$\left(\frac{\partial G}{\partial(\mathbf{q},\mathbf{p})}\right)^T \mathbf{J} \left(\frac{\partial G}{\partial(\mathbf{q},\mathbf{p})}\right) = \mathbf{J}, \qquad \text{here} : \mathbf{J} = \begin{pmatrix} \mathbf{0}_{n\times n} & \mathbf{E}_{n\times n} \\ -\mathbf{E}_{n\times n} & \mathbf{0}_{n\times n} \end{pmatrix}.$$

The symplectic maps form the group, preserve a given symplectic 2-form and its Lie algebra is the set of locally Hamiltonian vector fields. Then any composition of Hamiltonian flows lies in the group and eliminates another advantageous property of splitting methods. It is supposed that the total Hamiltonian is divided on simpler parts:

$$H = H_1(\mathbf{q},\mathbf{p}) + H_2(\mathbf{q},\mathbf{p}), \tag{8}$$

where H_1 represents the major dynamic Hamiltonian, H_2 corresponds to all remaining disturbances, $\mathbf{q}$ and $\mathbf{p}$ are generalized coordinates and momenta. If the general solution corresponding to H is complex and not efficiently evaluable in contrast to the solutions generated by H_1, H_2 separately, then the symplectic integration schemes can be used.

The simplest symplectic scheme of the first order which preserves Hamiltonian structure of the motion equations of a rigid body with a fixed point was obtained in the paper [3] by multiplying the perturbation H_2 by a periodic sequence of Dirac delta functions

$$H_{map} = H_1 + 2\pi\,\delta_{2\pi}(\gamma t)\,H_2, \tag{9}$$

where

$$\delta_{2\pi}(t) = \sum_{n=-\infty}^{\infty} \delta(t - n2\pi) = \frac{1}{2\pi} \sum_{n=-\infty}^{\infty} \cos(nt), \tag{10}$$

and γ is the mapping frequency, which is related to the step size h of the mapping $\gamma = \frac{2\pi}{h}$. Although each Hamiltonian $H_i (i = 1, 2)$ is separately integrable in the canonical Andoyer-Deprit variables, to achieve good performance for symplectic integration Wisdom and Touma used the components of the angular momentum vector in the body fixed coordinate frame instead.

As the second order algorithm accurate in step size, according to (7), the leapfrog scheme [1,6] can be generated for the Hamiltonian H divided into two parts. This scheme is given symbolically using Lie operator notation [7] :

$$e^{\frac{h}{2}H_1}\; e^{hH_2}\; e^{\frac{h}{2}H_1}. \tag{11}$$

The interpretation of this notation is that the operator $\mathrm{e}^{\frac{h}{2}H_1}$ means motion with respect to H_1 dynamics over the time step of length $h/2$. This is then followed by the operator e^{hH_2} meaning moving the system over the time step h assuming H_2 to be the Hamiltonian of the system. Finally, another time step of length $h/2$ is performed according to H_1 dynamics.

These three stages result in propagation the phase space trajectory corresponding to H over the time step h.

More advanced methods than the leapfrog scheme described can be constructed [8] using, for example, kernels of the form

$$\mathrm{e}^{U_1 h H_2}\mathrm{e}^{W_1 h H_1}\mathrm{e}^{U_2 h H_2}\mathrm{e}^{W_2 h H_1}\mathrm{e}^{U_3 h H_2}...,$$

where the U's and W's are determined by a conventional numerical integration formula. The W coefficients are proportional to the differences of abscissae and the U coefficients are weights from the formula in question. Then the well known Simpson's rule can be applied:

$$\mathrm{e}^{\frac{h}{3}H_2}\mathrm{e}^{hH_1}\mathrm{e}^{\frac{4h}{3}H_2}\mathrm{e}^{hH_1}\mathrm{e}^{\frac{h}{3}H_2}. \tag{12}$$

Methods constructed in this way have similar orders to the error of the associated numerical integration formula, but this applies only to the first order perturbations. Thus it is necessary that H_2 is small enough for the formula to be useful.

2. Motion of a free rigid body with a fixed point. To describe the angular dynamics of a rigid body with a fixed point it is assumed that the body is fixed in its mass center where the origin O of the body-fixed coordinate system XYZ is placed so that the principal coordinate axes coincide with the frame $OXYZ$. If the body angular motion is free from any external disturbances then the angular momentum vector is constant in inertial space. The following above characterizes the well-known Euler's case of motion of the rigid body with the fixed point. The kinetic energy of rotation of the body about the mass center is

$$H_E = \frac{1}{2}(\mathbf{M}\cdot\mathbf{I}^{-1}\mathbf{M}). \tag{13}$$

Here: $\mathbf{M} = \mathbf{I}\boldsymbol{\omega}$ is the angular momentum vector of the body in the coordinate frame $OXYZ$, $\mathbf{I} = \mathrm{diag}(I_1, I_2, I_3)$ is the inertia matrix with respect to the point O. As it was shown in [3], the Euler equations for the angular momentum $\mathbf{M}$ with respect to the body-fixed coordinate frame have the Poisson structure:

$$\dot{\mathbf{M}} = \left\{\mathbf{M}, \frac{\partial H_E}{\partial \mathbf{M}}\right\} = (\mathbf{M}\times\mathbf{I}^{-1}\mathbf{M}), \tag{14}$$

the dot over the variable designates the time derivative in the body-fixed frame.

Following (8)-(10), the Hamiltonian (13) is splitted into two parts

$$H_E = H_A + H_T. \tag{15}$$

Here H_A governs the motion of an axisymmetric body and H_T acts as a perturbation. In the paper [3] it was assumed that the body is nearly axisymmetric in the plane passing trough the first and second principal axes with $I_2 = I_1(1+\epsilon)$, $\epsilon \ll 1$. Under this assumption the Hamiltonian H_T is the small perturbation to H_A. Based on (13), those Hamiltonians are written in the form:

$$H_A = \frac{(M_1^2 + M_2^2)}{2I_2} + \frac{M_3^2}{2I_3}, \tag{16}$$

$$H_T = \frac{M_1^2}{2}\left(\frac{1}{I_1} - \frac{1}{I_2}\right). \tag{17}$$

However, Wisdom and Touma [3] suggested that the splitting (15) - (17) is valid not only for the nearly axisymmetric rigid body $\epsilon \ll 1$, but for more general mass distribution $\epsilon < 1$ as well. Note, that for both H_A and H_T the corresponding exact solutions still can be found, this allows to combine them into single symplectic scheme and avoid the use of elliptic functions. Those exact solutions are formulated in the next two subsections.

Case of the axisymmetric body. At first, the part of vector field of the Euler dynamic equations corresponding to the Hamiltonian H_A is considered. The Euler dynamic equations (14) become

$$\begin{aligned}
&\frac{d}{dt}M_1 = \big(\frac{1}{I_3} - \frac{1}{I_2}\big) M_2 M_3,\\
&\frac{d}{dt}M_2 = -\big(\frac{1}{I_3} - \frac{1}{I_2}\big) M_1 M_3,\\
&\frac{d}{dt}M_3 = 0.
\end{aligned}$$

This ODEs system can be taken as linear with respect to M_1 and M_2, because $M_3 = const$. Then the exact solution for the initial value problem on the time interval $[t_0, t]$ is given in the vector form:

$$\boldsymbol{M}(t) = [\mathbf{R}_Z(\alpha(t_0, t))]\boldsymbol{M}(t_0), \tag{18}$$

where

$$\alpha(t_0, t) = \left(\frac{1}{I_3} - \frac{1}{I_2}\right) M_3(t_0)(t - t_0), \tag{19}$$

and the matrix of rotation about the body axis Z is

$$\mathbf{R}_Z(\alpha(t_0, t)) = \begin{pmatrix} \cos\alpha(t_0, t) & \sin\alpha(t_0, t) & 0 \\ -\sin\alpha(t_0, t) & \cos\alpha(t_0, t) & 0 \\ 0 & 0 & 1 \end{pmatrix}. \tag{20}$$

Case of the triaxial body. The part of the vector field of the Euler dynamic equations corresponding to H_T under the assumption $\epsilon \ll 1$ is studied. The motion equations (14) are reduced to

$$\begin{aligned}
&\frac{d}{dt}M_1 = 0,\\
&\frac{d}{dt}M_2 = \left(\frac{1}{I_1} - \frac{1}{I_2}\right) M_1 M_3,\\
&\frac{d}{dt}M_3 = -\left(\frac{1}{I_1} - \frac{1}{I_2}\right) M_1 M_2,
\end{aligned}$$

On the time interval $[t_0, t]$ for the initial value problem these equations have the exact solution

$$\boldsymbol{M}(t) = [\mathbf{R}_X(\beta(t_0, t))]\boldsymbol{M}(t_0), \tag{21}$$

where

$$\beta(t_0, t) = \left(\frac{1}{I_1} - \frac{1}{I_2}\right) M_1(t_0)(t - t_0). \tag{22}$$

The rotation about X axis is given by the matrix

$$\mathbf{R}_X(\beta(t_0,t)) = \begin{pmatrix} 1 & 0 & 0 \\ 0 & \cos\beta(t_0,t) & \sin\beta(t_0,t) \\ 0 & -\sin\beta(t_0,t) & \cos\beta(t_0,t) \end{pmatrix}. \tag{23}$$

Thus, following the ideas of Wisdom and Touma [3], the splitting (16),(17) eliminates that the rigid body motion is represented as the sequence of rotations with two frequencies given in (19), (22). The combination of two such rotations can be used to construct the various symplectic schemes.

3. Leapfrog and Simpson symplectic schemes for a free rigid body. It is assumed that the numerical integration of equations (14) with the initial condition $\mathbf{M}(t_0) = \mathbf{M}_0$ is needed for the time interval $[t_0, t_N]$. Then the propagation formula for every time step $(i = 0, \ldots, N)$ is given by the nonlinear iterated mapping $S : \mathbf{M} \to \mathbf{M}$, $\mathbf{M} \in \mathbf{R}^3$

$$\mathbf{M}(t_{i+1}) = \big[\mathbf{P}(\mathbf{M}(t_i), h_i)\big]\mathbf{M}(t_i), \tag{24}$$

where $\mathbf{P}_{(3\times3)}$ is the transformation matrix combining a sequence of rotations, the time step is constant $h_i = t_{i+1} - t_i = h$, $i = 0, \ldots, N$. In the following subsections the leapfrog and Simpson schemes are generated to propagate the angular moment of the rigid body for the Euler case. The corresponding iterated mappings are symplectic in terms of the canonical Andoyer-Deprit variables.

Leapfrog scheme. Using Lie operator notation, leapfrog scheme (11) for symplectic integration of (14) is symbolically represented by

$$e^{\frac{h}{2}H_T}\ e^{hH_A}\ e^{\frac{h}{2}H_T}. \tag{25}$$

The scheme has the accuracy of $O(h^2)$. Based on (24), the transformation matrix of scheme (25) implies three steps

$$\mathbf{P}^{LS} = [\mathbf{R}_X(h/2), [\mathbf{R}_Z(h), \mathbf{R}_X(h/2)]], \tag{26}$$

where $[,]$ designates the product of two (3×3) matrixes. Hence, according to (16)-(23), matrix (26) has the components

$$P_{11}^{LS} = \cos\alpha_i, \qquad P_{12}^{LS} = -P_{21}^{LS} = \sin\alpha_i \cos\frac{\beta_i}{2},$$

$$P_{13}^{LS} = P_{31}^{LS} = \sin\alpha_i \sin\frac{\beta_i}{2}, \quad P_{22}^{LS} = (1+\cos\alpha_i)\cos^2\frac{\beta_i}{2} - 1,$$

$$P_{23}^{LS} = -P_{32}^{LS} = \frac{1}{2}(\cos\alpha_i + 1)\sin\beta_i, \quad P_{33}^{LS} = (1+\cos\alpha_i)\cos^2\frac{\beta_i}{2} - \cos\alpha_i.$$

The components depend on both $\alpha_i = \alpha(t_i, t_{i+1})$, $\beta_i = \beta(t_i, t_{i+1})$, i.e. the time step and the vector $\boldsymbol{M}(t_i) = (M_1(t_i), M_2(t_i), M_3(t_i))$.

Simpson scheme. To integrate (14), Simpson scheme (12) is written by using Lie operator

$$e^{\frac{h}{3}H_T}\ e^{hH_A}\ e^{\frac{4h}{3}H_T}\ e^{hH_A}\ e^{\frac{h}{3}H_T}. \tag{27}$$

The scheme has the accuracy of $O(h^3)$. Following (24), the matrix of scheme (27) is the sequence of five rotations

$$\mathbf{P}^{SS} = [\mathbf{R}_X(h/3), [\mathbf{R}_Z(h), [\mathbf{R}_X(4h/3), [\mathbf{R}_Z(h), \mathbf{R}_X(h/3)]]]]. \tag{28}$$

Taking into account (16)-(23), the components of matrix (28) are given by the formulas

$$P_{11}^{SS} = \cos^2\alpha_i - \sin^2\alpha_i \cos\frac{4\beta_i}{3},$$

$$P_{12}^{SS} = -P_{12}^{SS} = \frac{1}{2}\sin 2\alpha_i \cos\frac{\beta_i}{3}(1+\cos\frac{4\beta_i}{3}) - \sin\frac{\beta_i}{3}\sin\frac{4\beta_i}{3}\sin\alpha_i,$$

$$P_{13}^{SS} = P_{31}^{SS} = \frac{1}{2}\sin 2\alpha_i \sin\frac{\beta_i}{3}(1+\cos\frac{4\beta_i}{3}) + \cos\frac{\beta_i}{3}\sin\frac{4\beta_i}{3}\sin\alpha_i,$$

$$P_{22}^{SS} = (-\sin^2\alpha_i + \cos\frac{4\beta_i}{3}\cos^2\alpha_i)\cos^2\frac{\beta_i}{3} - \sin\frac{4\beta_i}{3}\sin\frac{2\beta_i}{3}\cos\alpha_i - \cos\frac{4\beta_i}{3}\sin^2\frac{\beta_i}{3},$$

$$P_{23}^{SS} = -P_{32}^{SS} = \frac{1}{2}\sin\frac{2\beta_i}{3}(-\sin^2\alpha_i + \cos\frac{4\beta_i}{3}\cos^2\alpha_i + \cos\frac{4\beta_i}{3}) + \sin\frac{4\beta_i}{3}\cos\frac{2\beta_i}{3}\cos\alpha_i,$$

$$P_{33}^{SS} = (\sin^2\alpha_i - \cos\frac{4\beta_i}{3}\cos^2\alpha_i)\sin^2\frac{\beta_i}{3} - \sin\frac{4\beta_i}{3}\sin\frac{2\beta_i}{3}\cos\alpha_i + \cos\frac{4\beta_i}{3}\cos^2\frac{\beta_i}{3}.$$

Here $\beta_i = \beta(t_i, t_{i+1})$, $\alpha_i = \alpha(t_i, t_{i+1})$ are given by (19), (22).

4. Computational experiments. In this section the leapfrog and Simpson symplectic schemes are tested against, obtained by Fehlberg [9], the fifth order Runge - Kutta method with six stages and constant step size. To setup integration the principal inertia moments are chosen $\mathbf{I} = \mathrm{diag}(40.5, 40.6, 50.0)(kg*m^3)$. The initial conditions are given for the angular velocity in the body fixed frame $\boldsymbol{\omega}(t_0) = (1.0, 0.0, 10.0)$ (deg/sec). At first, the leapfrog scheme integration results for $\boldsymbol{\omega}^{LS}(t)$ are represented on figures 1,2 for all the coordinates separately and on picture 3 as the phase space trajectory. The time step is $h = 0.1$ sec and the integration time is 600 seconds.

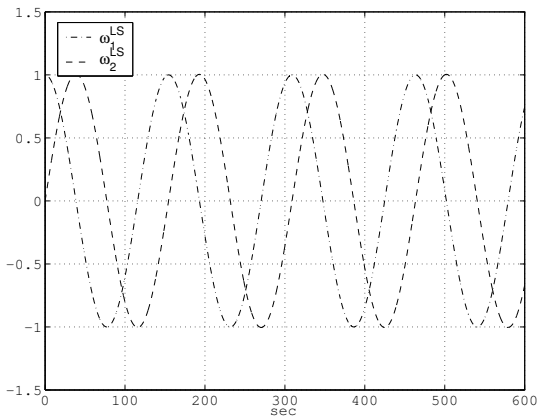

Fig. 1. Propagation of $\omega_1^{LS}(t)$ and $\omega_2^{LS}(t)$.

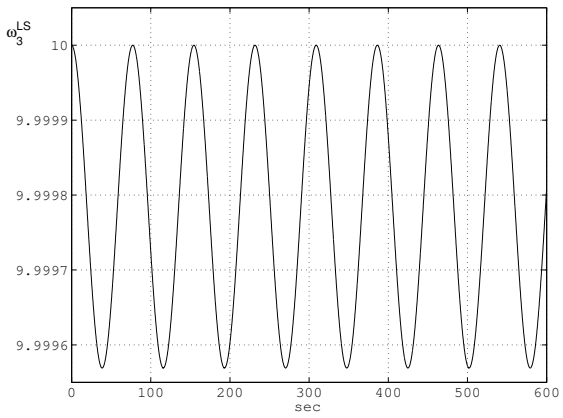

Fig. 2. Propagation of $\omega_3^{LS}(t)$.

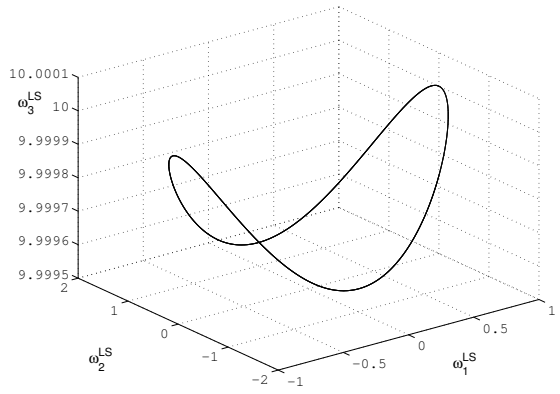

Fig. 3. The hodograph $\boldsymbol{\omega}^{LS}(t)$ in the phase space.

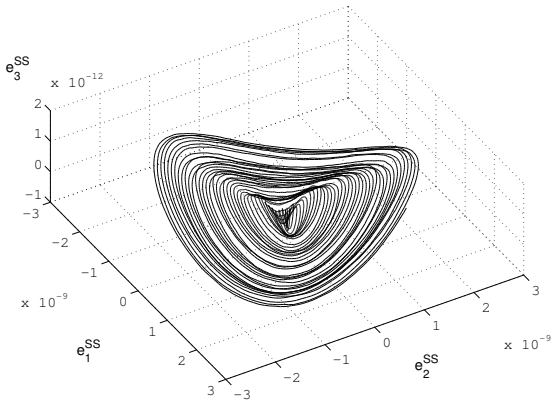

Fig. 4. The hodograph $\boldsymbol{e}^{SS}(t)$ in the phase space.

To compare the leapfrog "LS"and Simpson "SS"methods against the high order Runge-Kutta method "RK"on longer time intervals, the solutions obtained above are propagated up to 100 minutes, i.e. approximately for one orbital period for small satellite on low Earth orbit. Then the absolute error vectors

$$\mathbf{e}^{LS}(t) = \boldsymbol{\omega}^{RK}(t) - \boldsymbol{\omega}^{LS}(t), \qquad \mathbf{e}^{SS}(t) = \boldsymbol{\omega}^{RK}(t) - \boldsymbol{\omega}^{SS}(t),$$

are calculated and plotted on figures 4, 5 and 6, converted in (deg/sec). It can be noted, that these errors remain small for first 10 minutes of integration time. The difference between "LS"and "SS"integration results is also in agreement with the orders of these methods and the time step, i.e. the Simpson scheme has the smallest absolute error. It is shown that the absolute errors between "LS"and "RK"methods are in the band of order 10^{-6}. For the Simpson scheme the relative errors with respect to the Runge - Kutta results are in the smaller band of order 10^{-7}.

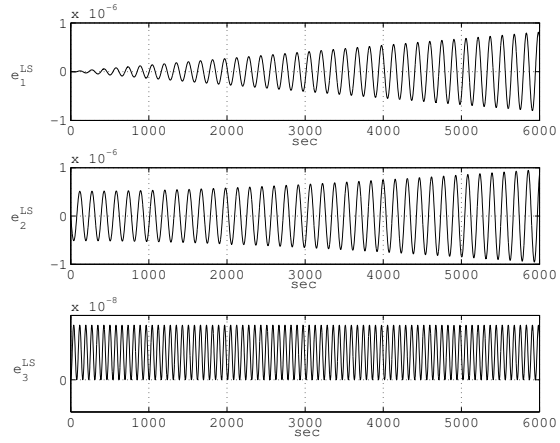

Fig. 5. Evolution of $e_i^{LS}(t)$ $(i = 1, 2, 3)$.

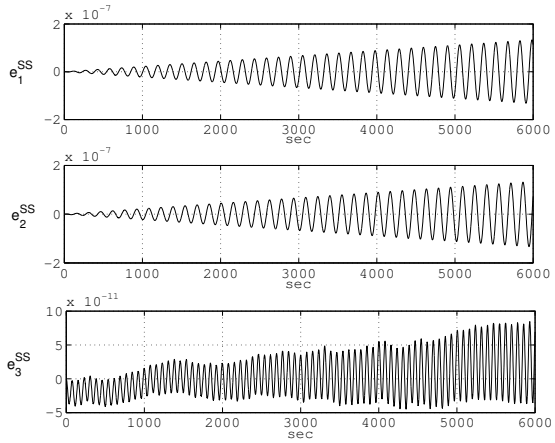

Fig. 6. Evolution of $e_i^{SS}(t)$ $(i = 1, 2, 3)$.

To demonstrate the error in the kinetic energy and magnitude of angular momentum vector, the deviations from the initial values

$$dH(t) = H(t) - H(t_0), \qquad dM(t) = |\mathbf{M}(t)| - |\mathbf{M}(t_0)|,$$

are plotted on figures 7 and 8 for all three integration methods. The energy deviations for "RK"and "SS"results are about the same order, that is hundred times smaller than for

"LS"scheme. The deviations in $|\mathbf{M}|$ for all three methods are staying in the band of order 10^{-13}.

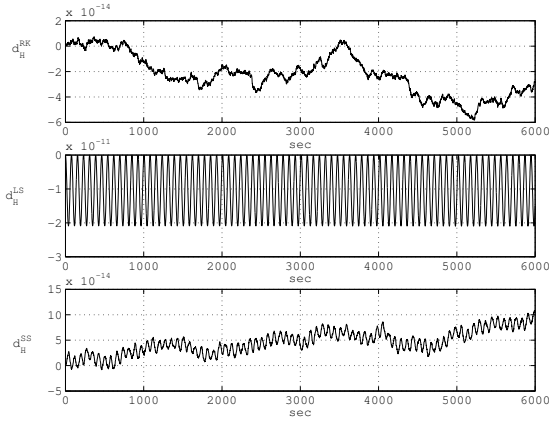

Fig. 7. The deviations in H for all three methods.

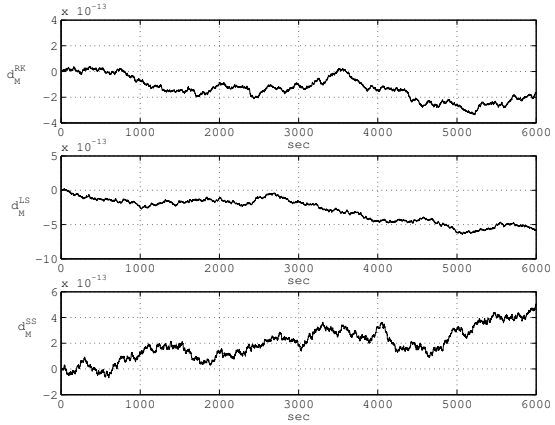

Fig. 8. The deviations in $|\mathbf{M}|$ for all three methods.

To study the dependence between the deviations in H and $|\mathbf{M}|$ and different time steps for the leapfrog, Simpson and Runge-Kutta methods, the maximum absolute values of deviations obtained above are calculated for the time step values

$$h = \{1.0, 0.8, 0.6, 0.4, 0.2, 0.1, 0.08, 0.06, 0.04, 0.02, 0.01\}.$$

The maximums are plotted on figures 9 and 10 against the time steps with decimal logarithmic scaling.

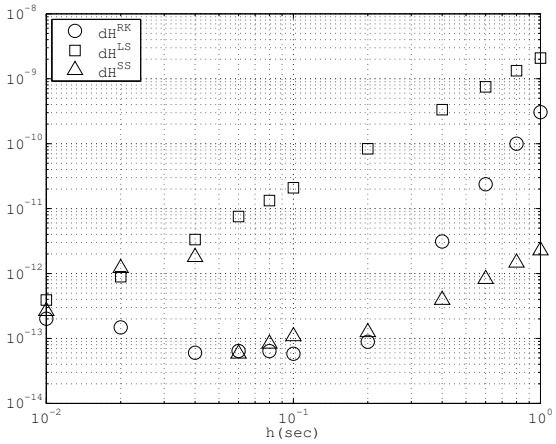

Fig. 9. The maximums of deviations in H.

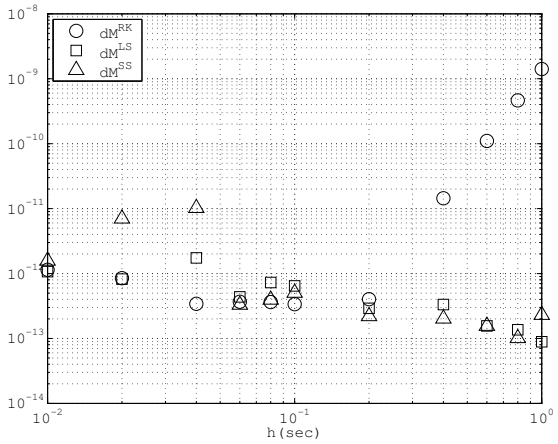

Fig. 10. The maximums of deviations in $|\mathbf{M}|$.

It is shown that the leapfrog scheme has the biggest energy deviation. The Simpson scheme has the smallest energy and $|\mathbf{M}|$ deviations in the range $h = \{1.0, 0.8, 0.6, 0.4\}$. The biggest $|\mathbf{M}|$ deviations are produced by the Runge-Kutta method for the same time step range. Thus, in this range the Simpson scheme outperforms the Runge-Kutta method. However, in the range $h = \{0.1, 0.08, 0.06\}$ the Simpson scheme and Runge-Kutta methods have the same order for deviations.

Finally, the number of computational operations per one integration step for the Runge-Kutta method "RK", leapfrog "LS" and Simpson "SS" schemes implemented for the Euler dynamic equations is calculated in table to estimate the speed of calculation. It is known that starting from the processor Intel 80 386 up to modern high frequency models the

trigonometric functions are included as commands for the co-processor. However the real processing time for arithmetic operations and calculation of trigonometric function relies upon the processor model. If this time can be precalculated on average for the processor in use, then one can select the fastest method from the table.

$\frac{Method}{operation}$	RK	LS	SS	$LS1$	$SS1$
$*/:$	99	18	30	33	55
$+/-$	63	6	10	12	20
sin		3	5		
cos		3	5		

If the integration time step is chosen small enough to put the approximations of the trigonometric functions $\sin\theta = \theta - 0.1(6)\theta^3$ and $\cos\theta = 1 - 0.5\theta^2$ for small values of θ in agreement with accuracy needed, then the number of operations is further reduced for the implementations of leapfrog "$LS1$" and Simpson "$SS1$" schemes. Hence, the leapfrog scheme and Simpson schemes are faster about 3 and 2 times correspondingly then the "RK"method.

1. *Wisdom J., Holman M.* Symplectic maps for the n-body problem // Astron. J. – 1991. – **102**. – P. 1528–1538.
2. *Susman G., Wisdom J.* Chaotic evolution of the solar system. – Science. – 1992. – 257 p.
3. *Touma J., Wisdom J.* Lie-Poisson integrators for rigid body dynamics in the solar system // Astron. J. – 1994. – **103**. – P. 1189–1209.
4. *Sanz-Serna J.M., Calvo M.P.* Numerical Hamiltonian problems. – Chapman and Hall, 1994. – 125 p.
5. *Mikkola S., Palmer P.L., Hashida Y.* A symplectic orbital estimator for direct tracking on satellites // J. of Astronautical Sciences. – 2000. – **48**, No.1. – P. 109–125.
6. *Kinoshita H., Yoshida H., Nakai H.* Symplectic integrators and their application in dynamical astronomy // Celest. Mech. Dyn. Ast. – 1991. – **50**. – P. 59–71.
7. *Koseleff P.V.* Relations among Lie formal series and construction of symplectic integrators // Applied algebra, algebraic algorithms and error correcting codes (Cohen G., Mora T., Moreno O., etc.). – AAECC-10. – New York: Springer-Verlag,1993. – P. 213–230.
8. *McLachlan R.I.* Composition methods in the presence of small parameters // BIT 35. – 1995. – P. 258–268.
9. *Fehlberg E.* Low order classical Runge-Kutta formulas with step size control and their application to some heat-transfer problems // Computing. – 1970. – **6**. – P. 61–71.

Institute of Appl. Math. and Mechanics of NASU, Donetsk, Ukraine
nat@iamm.ac.donetsk.ua

Received 20.07.03